

Tunable magnetic-field asymmetry of nonlinear mesoscopic transport: Field-effect controlled backscattering in a quantum wire

D. Hartmann, L. Worschech,* and A. Forchel

Technische Physik, Physikalisches Institut, Universität Würzburg, Am Hubland, 97074 Würzburg, Germany

(Received 4 August 2008; published 8 September 2008)

The nonlinear conductance of quantum wires has been studied in magnetic fields by applying an in-plane electric field via side gates. It has been found that magnetic-field asymmetries, defined as the change in the conductance induced by a change in the magnetic-field sign, become more pronounced the larger the gate voltage is and increase linearly with the bias voltage up to several millivolts. With an in-plane electric field the asymmetry can be tuned, the symmetry recovered, and also the asymmetry reversed, which is associated with a field-effect controlled backscattering of electrons.

DOI: [10.1103/PhysRevB.78.113306](https://doi.org/10.1103/PhysRevB.78.113306)

PACS number(s): 73.63.Nm, 72.10.Fk, 72.20.Dp

The momentum of electrons will undergo a change if a magnetic field is applied, which in turn modifies the transport properties of a conductor. According to the Onsager-Casimir symmetry relations, in the linear transport regime the conductance $G=I/V$ of a two-probe conductor, defined as the ratio of the current I through the conductor to the voltage V between the probes, remains unaffected for a reversal of an external magnetic field.^{1,2} Recently, it has been found that an odd part in the magnetic field of nonlinear I - V characteristics of mesoscopic metallic systems can exist, for which all spatial symmetries are broken.^{3,4}

Magnetic-field asymmetries of the conductance have been predicted for chaotic or diffusive systems with random electric interference effects and have been observed in different systems such as Aharonov-Bohm rings, quantum dots, and carbon nanotubes.⁵⁻¹⁰ As a result one observes fluctuations in the mesoscopic current, which were found analytically for arbitrary temperature, magnetic field, and interaction strength.¹¹ Mesoscopic fluctuations in the current density, which are linear in the sample voltage, result from random interference of the electron waves along the different paths through the sample with different local electron densities around scattering centers. Both the local electron density and the potential of scatterers can fluctuate due to Coulomb interaction.^{12,13} As a consequence, the nonlinear conductance can manifest itself as an odd function in the magnetic field which typically fluctuates from sample to sample. The appearance of nonlinear magnetoconductance was principally associated with electron-electron interaction⁴ or screening,³ which also effectively results in electron-electron interaction. Recently, even the interaction of different conductors was demonstrated to cause magneto-asymmetries.¹⁴ As boundaries of conductors can be described by a superposition of electron potentials, an interesting question arises as to whether or not the interaction of an electron in a conductor with its boundaries can give rise to an asymmetry in nonlinear mesoscopic transport. Here we demonstrate field-effect controlled magnetic-field asymmetries with tunable value and sign in quantum wires. The phenomenon is robust up to sample voltages of several 10 millivolts and points to switchable scattering at the boundaries of the quantum wires.

The magnetic-field asymmetries in the nonlinear transport regime were investigated for quantum wires (QWs) (Refs.

15–18) and are assigned to local backscattering within the one-dimensional (1D) channel.^{19–24} Such field-effect controlled asymmetry suggests that the nature of scattering processes can be switched from backscattering at potential fluctuations to specular scattering at the electrostatic potential induced by an in-plane electric field. Thus the backscattering of electrons can be electrically regulated via gates, which allows the control of magnetic-field asymmetries; i.e., we can tune the system in the nonlinear regime from $G(B) \neq G(-B)$ to $G(B)=G(-B)$.

The studied QWs were based on modulation doped GaAs/AlGaAs heterostructures with a two-dimensional electron gas (2DEG) located 80 nm below the surface. The carrier density and the mobility of the 2DEG determined from Hall measurements in the dark were $n=3.7 \times 10^{11} \text{ cm}^{-2}$ and $\mu=8.9 \times 10^5 \text{ cm}^2/\text{Vs}$ at $T=4.2 \text{ K}$. The QWs with *in situ* defined side gates were realized by electron-beam lithography and wet chemical etching. An electron microscopy picture of a QW and a scheme of the electric setup are shown in Fig. 1(a) as the left and right insets, respectively. Etched trenches, 170 nm wide and 90 nm deep, isolate the side gates from the QW channel. The current I through the QW was determined from the voltage drop $V_{\text{bias}} - V$ at a resistance $R=10 \text{ k}\Omega$ in series with the QW. The measurements presented here were performed at a temperature of 4.2 K. The magnetic field was directed perpendicular to the sample plane. Figure 1(c) shows the conductance conducted in the linear regime versus the gate voltage of a quantum wire. Such quantum wires show conductance quantization. The height of the steps in the studied quantum wires is reduced to values of up to 5% of $2e^2/h$ and associated with scattering.²⁵

First, we characterized several QWs using standard dc conductance measurements with equal voltages applied to both side gates. The conductance $G=I/V$, determined for a set of bias voltages in the range between 2.5 and 100 mV, versus magnetic-field strength ranging from -1.0 to 1.0 T are shown in Fig. 1(a). For applied bias voltages between 2.5 and 100 mV, the sample voltage, i.e., the voltage which drops along the device, ranges between 1.9 and 79 mV. For that measurement both side-gate voltages were set to 0.4 V. At low sample voltages (e.g., $V=1.9 \text{ mV}$) and zero magnetic field, the channel conductance exhibits a pronounced minimum attributed to weak localization of electrons. Initially,

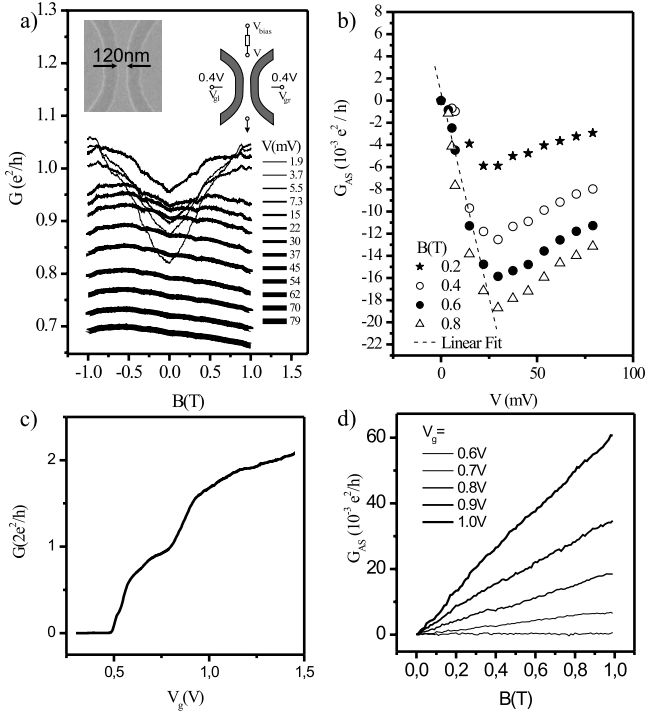


FIG. 1. (a) dc conductance $G=I/V$ as a function of magnetic field. Pronounced conductance asymmetries $G(-B) > G(B)$ are observed. Left inset: Electron microscopy image of a typical QW. Right inset: Schematic picture of the external measurement setup. (b) Asymmetric conductance G_{as} dependence on the voltage V for different magnetic fields. (c) Conductance versus gate voltage of a similar quantum wire fabricated from the same wafer. (d) Dependence of the asymmetric conductance G_{as} on the magnetic field for different $V_g = V_{gl} = V_{gr}$ for another wire fabricated from the same wafer. The asymmetry is small for low values of V_g .

the conductance for zero magnetic field, $G(B=0)$, increases for higher bias voltage. Then, the whole curves are shifted to lower values of the conductance. Similar observations were reported by Hornsey *et al.*²⁶ and interpreted in terms of a lowering of the potential barrier in the channel constriction by the applied bias. Above a critical value (~ 20 meV), this barrier lowering is compensated by increased electron-phonon scattering, which leads to a reduction in the conductance. One can see that small magnetic fields enhance the conductance of the QW, which is associated with a reduction in weak localization by breaking the time-reversal symmetry. Ramping up V , the weak localization effect vanishes approximately for $V > 30$ mV.^{27,28} Most remarkably, a magnetic-field asymmetry of the conductance $G(-B) > G(+B)$ in the observed magnetic-field range evolves with increasing V .

The asymmetric conductance $G_{as} = \frac{1}{2}[G(B) - G(-B)]$ as a function of the sample voltage V for a constant magnetic field is shown in Fig. 1(b). The magnetic-field asymmetry G_{as} increases almost linearly with the sample voltage up to a critical voltage $V \approx 20$ mV. Above this value, the linearity breaks down and the magnetic-field asymmetry decreases. As mentioned above for $V > 20$ mV, phonon scattering alters the conductance of the studied QW for zero magnetic field. Therefore, we conclude that electron-phonon-scattering

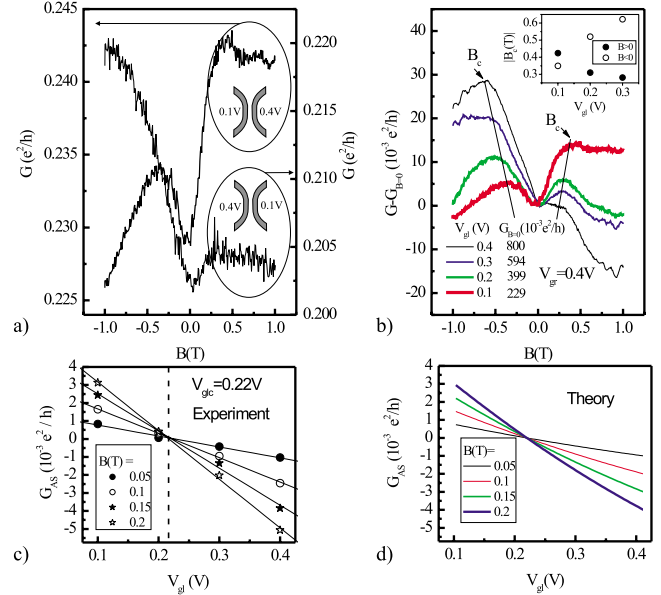


FIG. 2. (Color online) (a) dc conductance for two in-plane electric fields in opposite orientations. The bias voltage is set to $V_{bias} = 40$ mV. (b) $G - G_{B=0}$ for different side-gate voltages V_{gl} . V_{gr} is set to 0.4 V. The magnetic-field asymmetry can be tuned by an in-plane electric-field effect. (c) Experimental values of G_{as} vs V_{gl} . It is possible to influence G_{as} linearly by V_{gl} . Magnetic-field symmetry is recovered for $V_{gl} = 0.22$ V. (d) Computed lines as described by a modified Yacoby model for a wire with backscattering.

induced dephasing weakens also the cause of the magneto asymmetry.

The magnetic-field-induced asymmetry was studied in a series of a dozen QWs of similar size fabricated from the same wafer. The asymmetry was observed for all QWs. It was found that G_{as} fluctuates in both size and sign; e.g., in Fig. 1(b) G_{as} is negative for the QW studied first. In contrast, positive values of G_{as} were determined for another QW [Fig. 1(d)]. It was also found that G_{as} is larger the more positive the gate voltage is. In Fig. 1(d) G_{as} versus B is shown for different values of the gate voltage V_g applied equally to the side gates for a QW, which becomes conductive at about $V_g = 0.55$ V. Close to the threshold, the absolute value of G_{as} is negligibly small in the entire magnetic-field range. In contrast it reaches values of up to $G_{as} = 60 \times 10^{-3} e^2/h$ for a gate voltage of $V_g = 1.0$ V. This result points to the sidewalls of the QW as the origin of the asymmetry, since electrons can move closer to the sidewalls for an open wire with large gate voltages, whereas for small gate voltages the electrons pass through the QW more centrally.

Up to here, all measurements were performed with symmetrically wired side gates. To study the role of an in-plane electric field on G_{as} , we applied at one side gate a voltage which is, e.g., larger than the side-gate voltage applied to the adjacent gate and measured the conductance as a function of the magnetic-field strength. Then the gate voltages were exchanged and the measurement was repeated. One can see in Fig. 2(a) that for both orientations of the in-plane electric field with $V_{gl} = 0.1$ V and $V_{gr} = 0.4$ V and $V_{gl} = 0.4$ V and $V_{gr} = 0.1$ V, the curve evolutions with B differ, while the

overall dc conductances are comparable ($\sim 0.2e^2/h$). G principally increases apart from the weak localization dip from about 0.225 to 0.243 e^2/h for a left-side-gate voltage of 0.1 V and a right-side-gate voltage of 0.4 V (linked to the left axes). In contrast, the inverted gate configuration results in G decreasing from about 0.220 to 0.203 e^2/h (linked to the right axes) for the same sweep of B . To allow a more systematic analysis, the voltage at the right-side gate was fixed at 0.4 V with the other was tuned from 0.1 to 0.4 V. The corresponding curves are shown in Fig. 2(b). For better comparison, $G_{B=0}$ was subtracted from the magnetic-field-dependent conductance $G(B)$. In addition to the above-mentioned observation that for larger gate voltages applied to a QW (larger conductance) the asymmetry is more pronounced, it can be seen that with decreasing V_{gl} , the conductance $G - G_{B=0}$ is lowered for negative magnetic fields and raised for positive ones. In other words, G_{as} is negative for $V_{gl}=0.3$ V as well as $V_{gl}=0.4$ V and changes to a positive value for $V_{gl}=0.1$ V. Moreover, for small magnetic fields the magnetic-field asymmetry is almost compensated for $V_{gl}=0.2$ V. We determined G_{as} from these curves [Fig. 2(c)]. G_{as} decreases with increasing V_{gl} . An interesting fact is that G_{as} vanishes at $V_{gl}=0.22$ V for all presented magnetic-field values. Thus, the symmetry of the nonlinear QW transport can be recovered by a proper in-plane electric field.

We propose that the asymmetry of nonlinear transport in QWs is caused by in-plane electric-field controlled switching of electron backscattering at scatterers situated close to the hard sidewalls of the QW. Such an assumption is confirmed by the fact that the critical magnetic field B_c , at which weak localization (as indicated by arrows) sets in, changes with the magnetic-field direction and V_{gl} . As B_c is a measure of the average flux enclosed by backscattered trajectories,^{29,30} a change in B_c with the electric field reflects a change in the backscattered trajectories. In particular, with increasing number of scattering centers, the absolute value of B_c gets smaller. The dependence of $|B_c|$ on the left-side-gate voltage is shown in the inset of Fig. 2(b). For $B > 0$, $|B_c|$ decreases with increasing V_{gl} . In contrast, for $B < 0$, $|B_c|$ increases. Therefore, for $B > 0$, i.e., for the presently studied QW with electrons magnetically deflected toward the left hard wall of the QW, a lowering of V_{gl} lowers the number of scattering events. A complementary scenario is valid for $B < 0$. Here a lowering of V_{gl} seems to increase the electron backscattering. Taking into account that a smaller voltage at the left gate pushes electrons toward the right hard wall of the QW, it is reasonable to assume that defects at the sides of the QW are the origin of the scattering. On the other hand, backscattering at sidewall defects is smaller if the confining potential is created electrostatically so that electrons are pushed away. Gate electrodes are known to cause predominantly specular scattering.³¹

In Fig. 3 an overview sketch is shown. The QW is oriented along the x direction. The confining potential along the y direction is presented in the central part. The Fermi energy is labeled as E_F . If $V_{gl} > V_{gr}$ (left part), the effective potential $\Phi_{\text{eff}}(y)$ has such a form that electrons move closer to the left sidewall without a magnetic field. A magnetic deflection of electrons toward the left sidewall ($B > 0$) will then cause a

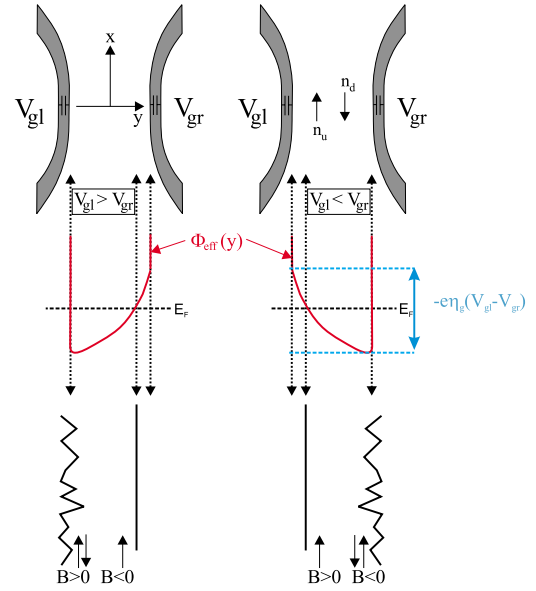


FIG. 3. (Color online) Scheme of Φ_{eff} for two in-plane electric fields with opposite orientations. Left: $V_{gl} > V_{gr}$. Electrons are scattered at the left channel boundary for positive magnetic fields. The transmission through the wire is large for negative magnetic fields. Right: $V_{gl} < V_{gr}$. Backscattering occurs predominantly at the right boundary, while scattering centers are reduced at the left side.

larger backscattering, as indicated by arrows, compared to a magnetic deflection of electrons toward the right sidewall ($B < 0$) as the electrostatic side-gate biasing prevents electrons from approaching the right sidewall. The potential profile and the scattering geometries for inverted side-gate voltages are shown in the center right and lower right graphs, respectively.

For a quantitative analysis of the field-effect controlled asymmetry, we have modified a model proposed by Yacoby *et al.*³² to describe the role of backscattering on the conductance in a quantum wire. In this frame, local electron densities $n_u(x)$ and $n_d(x)$ consider electrons moving in the wire up and down, respectively, as indicated in Fig. 3. Two scattering rates, Γ_{1D} and Γ_{2D} , describe the backscattering in the quantum wire when an up mover is scattered into a down mover (and vice versa) and between the 2DEG and the up/down movers, respectively. The parameter p considers different scattering rates, $\Gamma_{1D}(1+p)$ for up movers and $\Gamma_{1D}(1-p)$ for down movers. Solving the steady-state Boltzmann equations, $v \frac{\partial n_u}{\partial x} = n_u^{2D} \Gamma_{2D} + n_d \Gamma_{1D}(1-p) - n_u [\Gamma_{2D} + \Gamma_{1D}(1+p)]$, for up movers with the Fermi velocity v in contact with the up movers in the 2DEG (n_u^{2D}) and for the down movers, $v \frac{\partial n_d}{\partial x} = n_d^{2D} \Gamma_{2D} + n_u \Gamma_{1D}(1+p) - n_d [\Gamma_{2D} + \Gamma_{1D}(1-p)]$, one finds for $G_{as} = pev(n_u^{2D} + n_d^{2D}) / V(1 + \Gamma_{2D}/2\Gamma_{1D})$. Therefore, no asymmetry can occur if $\Gamma_{1D} = 0$ (backscattering is suppressed). To estimate G_{as} , one can consider that for a critical magnetic field $B = B_c = 0.4$ T with an in-plane electric field at the site of the quantum wire so large that $-e\eta_g(V_{gl} - V_{gr}) = E_F$ equals the Fermi energy $E_F = 15$ meV, with η_g as the gate leverage factor, all up movers are scattered specularly, i.e., $p = -1$. For a critical voltage at the drain of the QW $V_c = 2E_F/e = 0.03$ V, the barrier in the channel is

larger than the electrochemical potential of up movers. Thus no up movers can enter the quantum wire. From the offset of the conductance experiment and the subthreshold swing, we determined $\Gamma_{2D}/2\Gamma_{1D}=15\pm 4$ and $\eta_g\sim(5\pm 1)\%$. Therefore, $G_{as}\sim-(3.5\pm 1.1)\frac{e^2}{h\nu^2T}(V_{gl}-V_{gls})VB$, with V_{gls} as the left gate voltage for a symmetric wire. Corresponding computed lines are presented in Fig. 2(d) with $V_{gls}=0.22$ V for magnetic fields of $B=0.05, 0.1, 0.15,$ and 0.2 T. The experimental data are shown in Fig. 2(c). Having in mind that all parameters were determined from experiment in the linear regime, the model describes the experiment well. It should be mentioned that according to the model, the tunable asymmetry can exceed by far the symmetric part of the conductance.

In summary, we have investigated magnetic-field asym-

metries in the nonlinear transport regime of QWs. We observed linearity in the voltage and magnetic field of the magnetic-field asymmetry up to critical values. Furthermore we are able to control the asymmetry via side gates. The phenomenon was attributed to tunable backscattering of channel electrons at both channel sides. Such tunable magnetic-field asymmetry of nonlinear mesoscopic transport has the potential to serve as a mechanism for detection of magnetic fields in nanoscaled devices.

We thank M. Büttiker and M. L. Polianski for very useful discussions. We are grateful to M. Emmerling for expert technical assistance. This work was supported by the European Commission (IST-SUBTLE) and the state of Bavaria.

*worschech@physik.uni-wuerzburg.de

- ¹L. Onsager, Phys. Rev. **38**, 2265 (1931).
- ²H. B. G. Casimir, Rev. Mod. Phys. **17**, 343 (1945).
- ³D. Sánchez and M. Büttiker, Phys. Rev. Lett. **93**, 106802 (2004).
- ⁴B. Spivak and A. Zyuzin, Phys. Rev. Lett. **93**, 226801 (2004).
- ⁵L. Angers, E. Zakka-Bajjani, R. Deblock, S. Gueron, H. Bouchiat, A. Cavanna, U. Gennser, and M. Polianski, Phys. Rev. B **75**, 115309 (2007).
- ⁶R. Leturcq, D. Sanchez, G. Götz, T. Ihn, K. Ensslin, D. C. Driscoll, and A. C. Gossard, Phys. Rev. Lett. **96**, 126801 (2006).
- ⁷D. M. Zumbühl, C. M. Marcus, M. P. Hanson, and A. C. Gossard, Phys. Rev. Lett. **96**, 206802 (2006).
- ⁸C. A. Marlow, R. P. Taylor, M. Fairbanks, I. Shorubalko, and H. Linke, Phys. Rev. Lett. **96**, 116801 (2006).
- ⁹A. Löfgren, C. A. Marlow, I. Shorubalko, R. P. Taylor, P. Omling, L. Samuelson, and H. Linke, Phys. Rev. Lett. **92**, 046803 (2004).
- ¹⁰J. Wei, M. Shimogawa, Z. Wang, I. Radu, R. Dormaier, and D. H. Cobden, Phys. Rev. Lett. **95**, 256601 (2005).
- ¹¹M. L. Polianski and M. Büttiker, Phys. Rev. Lett. **96**, 156804 (2006).
- ¹²R. Landauer, Z. Phys. B **21**, 247 (1975).
- ¹³W. Zwerger, L. Bönig, and K. Schönhammer, Phys. Rev. B **43**, 6434 (1991).
- ¹⁴D. Sánchez and K. Kang, Phys. Rev. Lett. **100**, 036806 (2008).
- ¹⁵Ya. M. Blanter, F. W. J. Hekking, and M. Büttiker, Phys. Rev. Lett. **81**, 1925 (1998).
- ¹⁶R. de Picciotto, H. L. Stormer, L. N. Pfeiffer, K. W. Baldwin, and K. W. West, Nature (London) **411**, 51 (2001).
- ¹⁷S. Lal, S. Rao, and D. Sen, Phys. Rev. Lett. **87**, 026801 (2001).
- ¹⁸C.-T. Liang, M. Pepper, M. Y. Simmons, C. G. Smith, and D. A. Ritchie, Phys. Rev. B **61**, 9952 (2000).
- ¹⁹E. Abrahams, P. W. Anderson, D. C. Licciardello, and T. V. Ramakrishnan, Phys. Rev. Lett. **42**, 673 (1979).
- ²⁰P. W. Anderson, E. Abrahams, and T. V. Ramakrishnan, Phys. Rev. Lett. **43**, 718 (1979).
- ²¹L. P. Gorkov, A. I. Larkin, and D. E. Khmel'nitskii, JETP Lett. **30**, 228 (1979).
- ²²B. L. Al'tshuler, D. Khmel'nitskii, A. I. Larkin, and P. A. Lee, Phys. Rev. B **22**, 5142 (1980).
- ²³C. W. J. Beenakker and H. van Houten, Phys. Rev. B **38**, 3232 (1988).
- ²⁴G. Bergmann, Phys. Rev. B **28**, 2914 (1983).
- ²⁵F. Beuscher, L. Worschech, B. Weidner, and A. Forchel, Physica E (Amsterdam) **7**, 772 (2000).
- ²⁶R. I. Hornsey, A. M. Marsh, J. R. A. Cleaver, and H. Ahmed, Phys. Rev. B **51**, 7010 (1995).
- ²⁷H. van Houten, B. J. van Wees, M. G. J. Heijman, and J. P. André, Appl. Phys. Lett. **49**, 1781 (1986).
- ²⁸H. Linke, J. P. Bird, J. Cooper, P. Omling, Y. Aoyagi, and T. Sugano, Phys. Rev. B **56**, 14937 (1997).
- ²⁹K. Nakamura, D. C. Tsui, F. Nihey, H. Toyoshima, and T. Itoh, Appl. Phys. Lett. **56**, 385 (1990).
- ³⁰C. W. J. Beenakker and H. van Houten, Solid State Phys. **44**, 1 (1991).
- ³¹H. van Houten, B. J. Wees, J. E. Mooij, C. W. J. Beenakker, J. G. Williamson, and C. T. Foxon, Europhys. Lett. **5**, 721 (1988).
- ³²A. Yacoby, H. L. Stormer, N. S. Wingreen, L. N. Pfeiffer, K. W. Baldwin, and K. W. West, Phys. Rev. Lett. **77**, 4612 (1996).